

Synthesis, Characterizations, Antioxidant and Antibacterial Applications of Silver-incorporated Pectin-based Nanogel

Deepak Ram¹, Dr. Rohini Dharela^{2*}

¹Department of Chemistry, School of Sciences, A P Goyal Shimla University, Shimla, Himachal Pradesh, India-171013, raodeepak429@gmail.com,

²Department of Chemistry, School of Sciences, A P Goyal Shimla University, Shimla, Himachal Pradesh, India"-171013, rohinidharela@gmail.com,

Corresponding Author: Rohini Dharela*

*Department of Chemistry, School of Sciences, A P Goyal Shimla University, Shimla, Himachal Pradesh, India-171013, rohinidharela@gmail.com

ABSTRACT

A multipart approach was used to prepare composites of pectin-grafted-acrylamide (AgPAm) copolymer nanogel (Ngl) with silver incorporation. The characterization of the synthesized nanogel was subjected to studies, including FT-IR, XRD, and DSC analyses, as well as a swelling study to get evidence for successful synthesis and determine the end uses. The XRD evaluation showed a prominent peak for silver metal, emphasizing the successful synthesis. The FTIR analysis confirmed the crosslinking in the nanogel, while DSC was used to measure the changes in physical properties along with time over temperature.

The silver-incorporated nanogel was thereafter subjected to antimicrobial studies. Antibacterial analyses carried out against two different bacteria, i.e., gram negative and gram positive, showed a desirable inhibition zone of silver-incorporated nanogel, with a positive control (azithromycin, a known antibiotic) observed in this bacterial activity. The antioxidant assay showed that AgPAm inhibited free radical formation by up to 82%.

Keywords: Nanogel composite, antibacterial activity, and antioxidants activity.

1. INTRODUCTION

Nanotechnologies are gaining popularity as an interdisciplinary area of study due to their major characteristics in fields such as medicine, agriculture, physics, etc. Nanomedicines is a fascinating subject in the nanotechnology field for introducing innovative anticancer medications [1]. Nanomedicines offer effective therapeutic options for various malignancies and infectious disorders. Current antimicrobial medicines can control microorganism disease, however, they are ineffective due to drug resistance and environmental risk [2]. For this purpose, polymer composites such as the synthesized copolymer AgPAm have specific size-determine properties such as a substantial surface area and biocompatibility, making them attractive for antimicrobial applications, which can also have anticancer effects [3]. In their study, AgPAm had excellent antimicrobial activity against various microbes [4]. Hence, a new system including biomaterials such as pectin and its composite with AgPAm for the evaluation of antibacterial, and anticancer activities has been designed in this research work.

The plants include a variety of phytochemicals, including terpenoids, alkaloids, flavonoids, etc., which can help scavenge free radicals [5]. Pectin is the main component of the intermediate layer and is absorbed into the cell wall by vesicles formed by exocytosis in the Golgi apparatus [6,7]. When commercialized, it is a white to light brown powder usually obtained from citrus fruits. It is used as an agent in foods such as jams and jellies, as well as sweeteners, medicines, and stabilizers in fruit juices [8].

Among nanocarriers, naturally produced nanoparticles of polymeric substances, especially pectin, are efficient, inexpensive, and sustainable for the environment [9]. The growing interest in biocompatible, biodegradable, and non-toxic nanomaterials has accelerated research into the production of novel polymer nanomaterials [10-12]. Nanogels are special types of biomaterials considered to have a three-dimensional structure formed from physically and chemically crosslinked, soft hydrophilic macromolecular chains that may swell by holding a larger amount of water without dissolving while maintaining the integral structure [13]. Pectin significantly enhances the performance of nanogels, requiring chemical modifications to the polymer, such as crosslinking [14-20].

In the present work, the use of the crosslinking agent N,N-methylenebisacrylamide (MBA) with a natural polymer, namely pectin (Ptn), could achieve better properties in these polymers [21,22]. The goal of this work is the preparation of AgPAm composites with structural and morphological characterization and the study of their antibacterial and antioxidant properties. In fact, it appears that the copolymerization is due to the existence of Ptn molecules crosslinked to MBA through the synergic effect between components, as well as the high electrical conductivity and electrostatic interactions arising from active functional groups with a high ability to remove metal ions and microbes. The presence of silver metals in the synthesised nanogel helps facilitate the diffusion of molecules into cells, enhancing their antibacterial and antioxidant activity.

2. EXPERIMENTAL PARTS

Abbreviation: Ptn (Pectin), AAm (Acrylamide), MBA (N,N-Methylenebisacrylamide), (DW) Distilled water, APS (Ammonium persulphate), SDS (Sodium Dodecyl Sulphate), AgPAM[Silver-incorporated pectin-grafted-Acrylamide], and Nanogel (Ngl)

2.1. Materials

Pectin (Ptn) [Himedia Laboratories], Silver Nitrate (mw 169.87) [Avantor Performance Materials India Limited], Acrylamide monomer (AAm, 99%, mw 71.08) [Loba ChemiePvt. Ltd.], N,N-Methylene-bisacrylamide crosslinker (MBA, 99%, mw 154.17) [Loba ChemiePvt. Ltd.], Ammonium persulfate initiator (APS, 99%, mw 228.19) [Loba ChemiePvt. Ltd.], and Sodium Lauryl Sulphate/Sodium Dodecyl Sulphate (Needle shape extra pure, 91%, mw 288.38) [Loba ChemiePvt. Ltd.], all of these chemicals were purchased from Arun Chemicals, 14-U, A Jawahar Nagar, Delhi.

Sodium hydroxide (mw 40) [Thermo Fisher Scientific India Pvt.Ltd.], Methanol (99.8% mw 32.04) [Loba ChemiePvt. Ltd.], Sonicator (Digital Ultrasonic Cleaner, 80W), and Electronic Balance BL 220H, which has a capacity of 220 g and readability of 0.001 g (Shimadzu Corporation Japan), were provided by Alakh Prakash Goyal Shimla University H.P.

2.2. Method of Synthesis

To prepare an AgPAM nanogel, 10 ml of distilled water (DW) and 1 g of pectin powder were merged in a 100 ml beaker, stirred continuously, and then added to 0.15 g of NaOH and mixed. Add 0.015 g of APS, 0.500 g of AAm, and 0.015 g of MBA to another 100-ml beaker with 10 ml of distilled water and stir thoroughly. Mix the solution of both beakers together, and then add 0.01 g of SDS (surfactant) and 0.021 g of AgNO₃ solution (with 5-ml of distilled water) and continue stirring with a magnetic stirrer for 15-20 minutes at room temperature to make a homogeneous solution. After obtaining a homogeneous solution, keep the mixture in an ultrasonic sonicator for proper mixing at a temperature of 65-70 °C for 2-3 hours to proceed with the reaction and carry out the crosslinking.

After the crosslinking reaction, a gel-like substance was obtained through extraction with methanol. The extracted substance was dried in a hot air oven at 40 °C for 72 hours without disturbing. The dried substance was thus obtained in the form of a film that was named AgPAM (silver-incorporated pectin based acrylamide copolymerized) nanogel, as shown in **Figures 1 (a), (b)** and **Figure 2**.



(a) In the swollen form

(b) In the dried form

Figure 1. Represents (a) and (b) of the synthesized AgPAM-based nanogel.

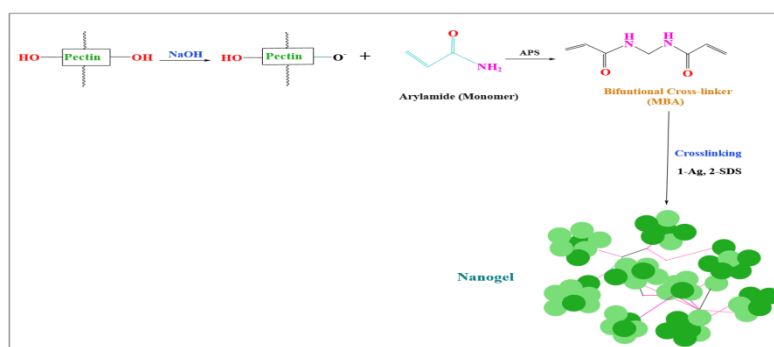


Figure 2. A schematic representation of nanogel's synthesis method.

3. ANTIBACTERIAL ACTIVITY

The antibacterial property of the synthesized nanogel was determined by Luria bertani agar disc diffusion, in which a filtered disc was saturated with the compound and placed on the surface of inoculated agar plates. The nanogel was diluted in DMSO to a 20 mg/mL solution and sterilized using a 0.22 μm Minisart syringe filter.

The antibiotic activity against four standard bacterial species, *Pseudomonas aeruginosa* (ATCC), *Escherichia coli* (ATCC), *Staphylococcus aureus* (ATCC), and *Streptococcus mutans*, was studied using the agar disc diffusion process. The antimicrobial study was examined at two distinct doses. Use a 90-mm Petri dish on each side and a 6-mm diameter sterile paper disk impregnated with 20 μL of synthetic nanogel solution, placed on the inoculated agar plate, and incubated at 37 $^{\circ}\text{C}$ for 17-19 hours [23]. The antibacterial activity of the nanogel was compared with the known antibiotic azithromycin (10 $\mu\text{g}/\text{disc}$) as a positive control and DMSO (20 $\mu\text{L}/\text{disc}$) as a negative control [24]. Using a Vernier scale in mm for measuring the estimated diameter of the zone of inhibition around the discs on the surface of the plates.

4. ANTIOXIDANT ACTIVITY

DPPH is a free radical with good stability that is frequently used to evaluate the capacity of an antioxidant component to remove radicals. The assessment of DPPH scavenging activity was conducted using the procedure outlined by Brand-Williams et al. (1995), with some modifications [25]. A solution of 1,1-diphenyl-2-picrylhydrazyl (DPPH) in methanol with a concentration of 0.004% was utilized. A 517 nm wavelength antioxidant reduces the concentration of DPPH, and over time, the absorption diminishes. The underlying principle of this technique is the decrease in DPPH concentration in a methanol solution, which is caused by the conversion of DPPH into its non-radical form in the presence of a hydrogen-donating antioxidant [26].

4.1. Preparation of Stock Solutions for the Sample

Measure out 1 gram of synthesized nanogel material. Then, pour 25 ml of methanol (99% purity) into the mixture. Finally, tightly cover the sample with aluminium foil. Once the sample is properly covered, place it in a water bath set to shake at a speed of 100 rpm. Let the sample remain in the water bath for a duration of 2 to 3 hours, maintaining the temperature at the level of the related room. Apply the sample to centrifugation at a rate of 6000–8000 rpm for a duration of 15 minutes, followed by filtration of the solution using filter paper. Prepare a series of solutions with volumes of 1 ml, 2 ml, 3 ml, 4 ml, and 5 ml, make up 10 ml by combining methanol (99%) with the extracted solution and additional methanol. Extract 1 ml from each solution and combine it with 3 ml of DPPH solution in each measured sample. Prepare each solution by adding up to 10 ml of 99% methanol. Store the samples in a dark environment for a period of 30 to 40 minutes.

4.2. Preparation of 1 M of DPPH Solution

To prepare the DPPH solution, mix 5 mg of DPPH with 100 ml of 99% methanol. Make sure to cover the DPPH solution with aluminium foil and keep it in a cool and dark place [27].

5. CHARACTERIZATION OF SYNTHESIZED NANOGEL

The analysis of the synthesized sample was done by different instruments, described as follows. The elemental compositions of the sample were analyzed by Energy Dispersive X-Ray (EDX, JSM 6490 LV, JEOL, Japan). The Fourier Transform Infra-Red (FTIR) spectra were reported between wavenumber ranges of 400-4000 cm^{-1} as a KBr pellet by a FTIR spectrometer (Nicole 6700, Thermo-Scientific, USA). X-ray diffraction (XRD) measurement was performed at a rate of 10 $^{\circ}/\text{minute}$ using an X-ray diffractometer (D8 Advance Eco, Bruker, Germany). DSC is a thermal analytical instrument that measures how the physical properties of a sample change along with temperature over time using the DSC thermogram [Setaram Instrumentation, Model D649, (temp 700 $^{\circ}\text{C}$ to 170 $^{\circ}\text{C}$), Russia].

6. RESULTS AND DISCUSSIONS

6.1. Fourier Transform Infrared Spectroscopy

The FT-IR spectra of AgPAm were recorded in the wavenumber range of 400-4000 cm^{-1} using an FTIR spectrometer (Nicole 6700, Thermo-Scientific, USA), as shown in **Figure 3**. The FT-IR spectrum of the synthesized nanogel revealed a broad band at 3299.12 cm^{-1} that was observed due to the stretching of O—H. The band at 2927.89 cm^{-1} was observed due to the asymmetric vibration of CH_2 and C—H [28]. Amide absorption bands were detected at 1657.03 cm^{-1} (amide I, stretching due to C=O) and 1325.83 cm^{-1} (amine II, stretching due to C—N). In addition to the characteristic band of the biopolymer, there are peaks located at 1228.91 cm^{-1} , 1142.43 cm^{-1} , and 1094.88 cm^{-1} , respectively, corresponding to the stretching of C—O evidence in the presence of the crosslinker [29]. The absorption bands around 960.85 cm^{-1} and 855.27 cm^{-1} represent out-of-plane bending and stretching caused by aromatic rings. Hence, it could indicate that the carboxyl and hydroxyl groups (methylated and acetylated) of the Ptn participate in the crosslinking reaction.

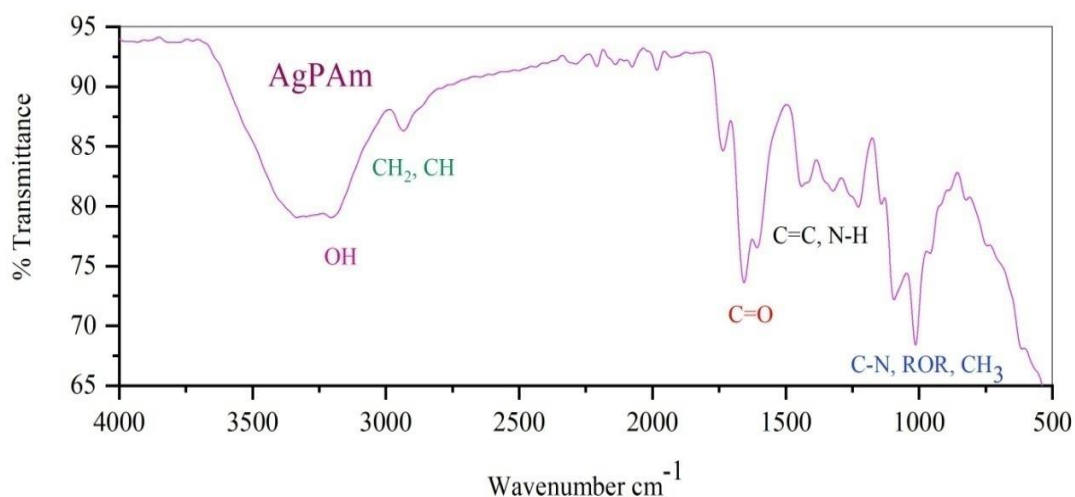


Figure 3. FTIR spectrum of synthesized AgPAm nanogel.

6.2. Differential Scanning Calorimeter

DSC is a thermal analytical instrument that measures how the physical properties of a sample change along with temperature over time. The result of the sample was obtained over a temperature range of 25 °C to 350 °C and a heating rate of 10 °C/min using the DSC thermogram [Setaram Instrumentation, Model D649, (temp 700 °C to 170 °C), Russia]. The glass transition (T_g) at about 40 °C is shown to have caused a baseline shift in the initial DSC scan of the Ngl heating, which is followed by an endotherm related to water evaporation. [30].

Two endothermic peaks can be seen in the thermogram at around 52.49 to 110.27 (°C) and 203.8 to 547.4 (s) and 130.97 to 162.49 (°C) and 671.06 to 859.8 (s), respectively, which indicate an endothermic reaction caused by the “melting” of the Ngl. [31]. After quench-cooling, a second heating scan was performed, and in such a scan, an exothermic peak was observed at 243.06 to 267.45 °C and 341.0 to 1486.0 (s) due to an exothermic reaction by “crystallization” (see DSC curve **Figure 4**). The nanogel shows some drift at the baseline due to thermal degradation. The T_g of Ngl was expected to be higher than that in the first scan due to the fact that water acts as a plasticizer and has flexibility, but was not detectable in the second scan. This behaviour corresponds with a polymeric sample and the individual T_g behaviours of its components. Nanogel polymers may exhibit varying thermal properties depending on the Ptn chain, which can affect the molecular weight and, as a result, the physicochemical properties of the compound, such as viscosity.

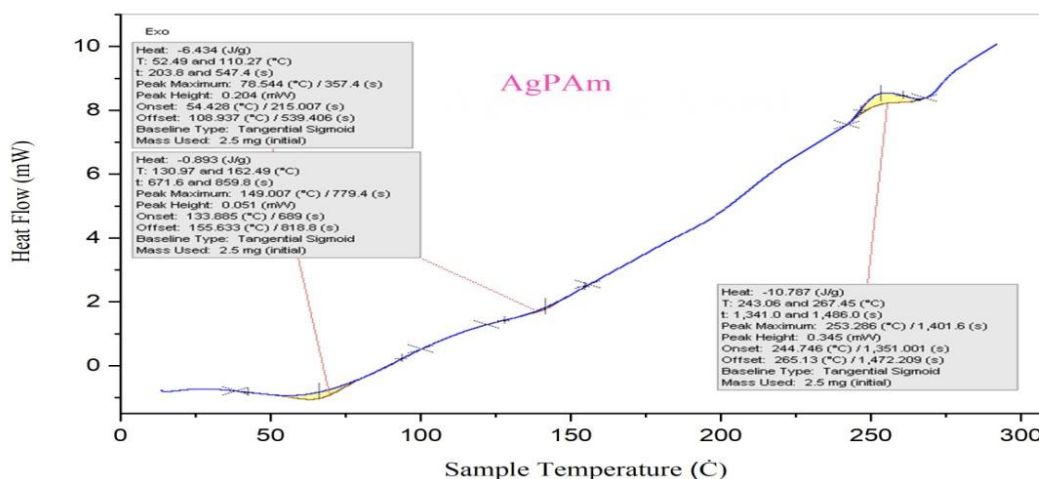


Figure 4. DSC analyses of AgPAm nanogel.

6.3. X-ray Diffraction

The crystal structure and size of the silver-incorporated nanogel were evaluated using an X-ray diffractometer (D 8 Advance Eco, Bruker, Germany), as depicted in **Figure 5**. The XRD analysis of the synthesized sample indicates diffraction peaks at $2\theta = 27.97, 32.34,$ and $46.38,$ respectively. The XRD spectrum indicated that the synthesized silver-incorporated nanogel is crystalline in nature and exists in nanocrystal form when compared to the reference. Peaks can be attributed to pure silver planes (131), (420), and (462) based on the face-centred cubic structure [32]. The structure showed more clearly planed peaks, as per the standard JCPDS [33], which can be attributed to the presence of Ptn molecules and hydrogen bonding by macromolecules that cause more regular chain rearranging in the copolymer. As a result, the synthesized nanogel's XRD peaks display more prominently. The Debye-Scherrer equation [34] was used to calculate the average particle size based on the results of the XRD study, taking into account the peaks at degrees.

$$D = 0.9\lambda / \beta \cos\theta, (\beta = \pi \times \text{FWHM}/180)$$

Where ‘λ’ is the wavelength (1.541 Å), FWHM (full width at half maximum), ‘θ’ is the diffraction angle, and ‘D’ is the diameter of particle size. The value of ‘d’ is calculated using Bragg’s Law.

$$n\lambda = 2d\sin\theta.$$

The average diameter of the synthesized nanogel was estimated from the Scherrer equation at 64 nm, as shown in **Table 1**. This result indicates that the biomaterial has a nano-sized structure.

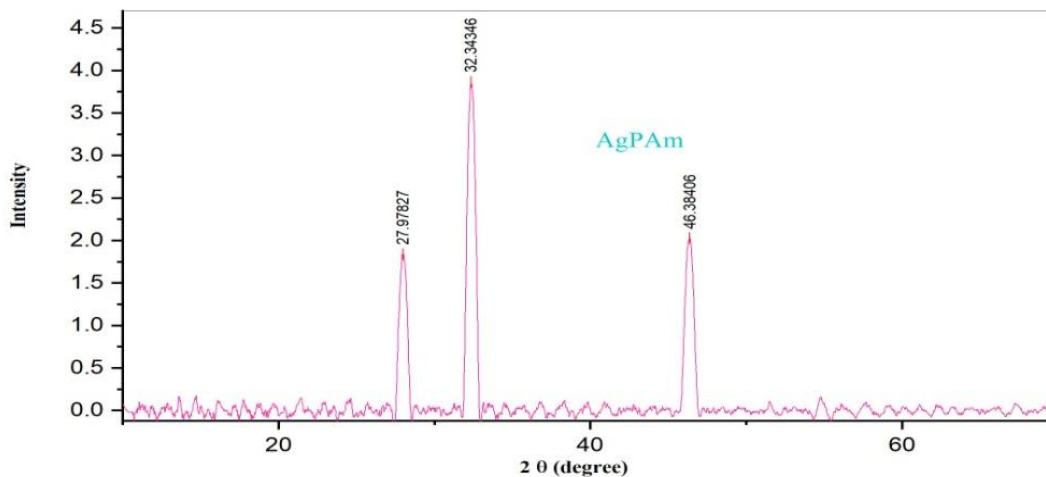


Figure 5. XRD analytical graph of AgPAm Ngl.

Table 1. Calculation of particle size by using XRD of synthesized nanogel.

Peak Position (2 θ)	Theta	FWHM	Crystallite Size D (nm)	d Spacing
27.9782	13.9891	1.2735	62.3728	3.1873
32.3434	16.1717	1.2254	64.8205	2.7664
46.3840	23.1920	1.2018	66.0928	1.9565

7. ANTIBACTERIAL ACTIVITY

The antibacterial activity of the synthesized nanogel was examined by Luria bertani agar disc diffusion with two types of bacteria, gram-negative (*Pseudomonas aeruginosa*, *Escherichia coli*) and gram-positive (*Staphylococcus aureus*, *Streptococcus mutans*). The antibacterial properties of the nanogel at two distinct concentrations (10 and 20 µg/disc) were compared with a known antibiotic, azithromycin, as a positive control. The antibacterial images are displayed in **Figure 6**, and the obtained results are reported in **Table 2**. The antibacterial investigation indicated a more favourable inhibition zone, particularly in *Pseudomonas aeruginosa*. There was no influence of the positive control (azithromycin) on bacterial activity, but synthesized silver-based nanogel produced significantly better results. Because of its resistance to azithromycin and increased hydrophobicity, it exhibits greater antibacterial action. As can be seen, synthesized nanogel’s antibacterial activity grows from its redox and dopant properties, which resist bacteria via electrostatic interaction through the cellular wall of the bacteria [35-38].

Increased hydrophobicity brings out more antibacterial properties. The result can be attributed to the fact that the presence of silver and pectin, which contain hydroxylic, carboxylic, and esteric groups, facilitates the diffusion of nanoparticles inside bacterial cell membranes, thereby inhibiting cell growth by damaging its cytoplasm. The antibacterial

activity reveals that the synthesized Ngl is resistant to azithromycin. The AgPAm molecule improves the penetration of acrylamide chains into the bacterial cell wall, enhancing the influx of the desired entity into the interior of the cell and the destruction of cell cytoplasm, leading to better activity for silver-incorporated nanogel than the traditional drugs.

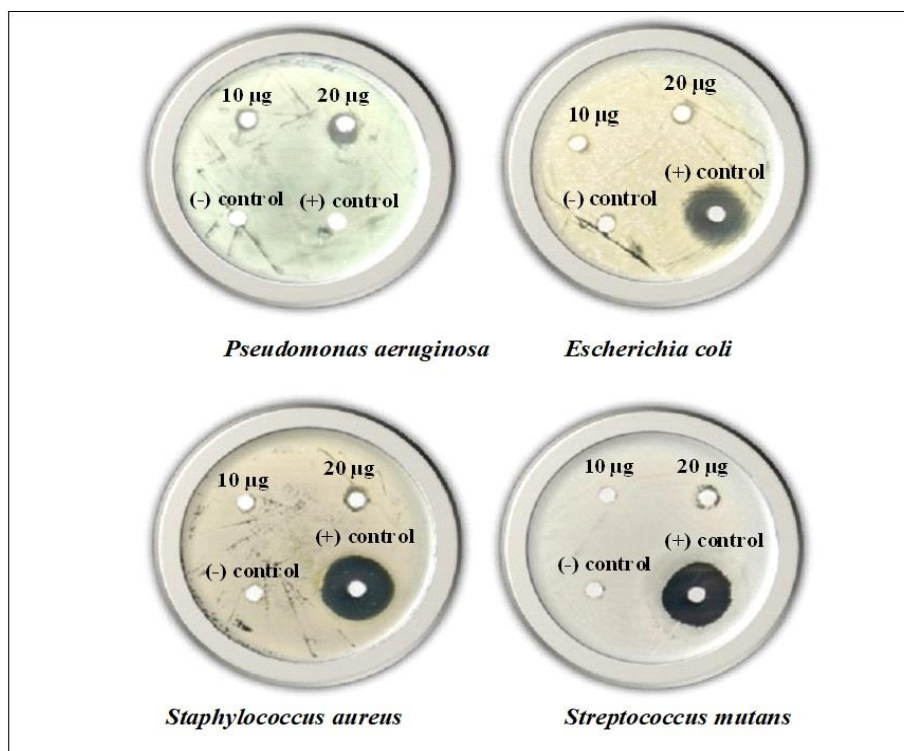


Figure 6 The images are related to the antibacterial activity of nanogel.

Table 2. The zone of inhibition of antibacterial activity of nanogel.

BACTERIAS →		GRAM-NEGATIVE		GRAM-POSITIVE	
		<i>Pseudomonas aeruginosa</i>	<i>Escherichia coli</i>	<i>Staphylococcus aureus</i>	<i>Streptococcus mutans</i>
Samples	Conc.	Zone of inhibition		Zone of inhibition	
AgPAm	10 µg	5 mm	0 mm	7 mm	0 mm
	20 µg	9 mm	0 mm	11 mm	11 mm
Azithromycin	10 µg	0 mm	19 mm	23 mm	21 mm

8. ANTIOXIDANT ACTIVITY

8.1. Procedure for Antioxidant Activity

This method was employed to acquire samples of prepared nanogel at concentrations ranging from 50, 100, 150, 200, and 250 µg/ml in intervals of 5 mg/ml. The nanogel test was diluted in distilled water and subjected to sonication for 10 minutes to prepare the working solutions. The solutions were kept at room temperature for a period of 30 minutes. The study was carried out using a Synergy H1-Multi plate reader instrument (Biotek) [39-41]. Ascorbic acid was used as the positive control or standard, whereas methanol was used as the blank. The spectrophotometer measured the absorbance of the DPPH solution at its peak wavelength of 517 nm. The studies were conducted a total of three times, and the percentage of scavenging activity was measured using the equation provided by reference [42].

$$[(\text{Absorbance control} - \text{Absorbance sample}) / \text{Absorbance control}] \times 100.$$

8.2. DPPH Scavenging Assay

Measurement of antioxidant activity using the DPPH test. The antioxidant activity of the AgPAm nanogel was evaluated using the DPPH radical scavenging experiment. The samples were generated at a concentration of 5 mg/ml for a nanogel based on silver. The concentrations of the synthesized nanogel extract were prepared at 50, 100, 150, 200, and 250 µg/ml, respectively. As a positive control, doses of ascorbic acid ranging from 20 to 140 µg/ml were utilized [43]. We detected a notable change in the ability of the investigated materials to eliminate DPPH radicals. There was a direct correlation between the dosage administered and the exhibited scavenging capacity. The scavenging capacity of the synthesized Ag-based nanogel at a concentration of 50 µg/ml was measured to be 15.18 [44]. The highest scavenging capacity was recorded at 81.34 at a concentration of 250 µg/ml, as depicted in **Figure 7**, when the concentration was raised to 250 µg/ml. The DPPH radical scavenging experiment was used to evaluate the antioxidant properties of

synthesized nanogel. The samples were generated at concentrations of 50, 100, 150, 200, and 250 $\mu\text{g/ml}$ for AgPAm. Ascorbic acid was used as a positive control, with values ranging from 20 to 140 $\mu\text{g/ml}$. The work shows that the synthesized AgPAm has antioxidant capabilities [45]. The investigated samples exhibited a significant alteration in their capacity to scavenge DPPH radicals. There was a clear relationship between the dosage given and the scavenging ability demonstrated. The antioxidant activity of a material is based on its ability to provide active hydrogen atoms that can effectively neutralize free radicals and decrease the levels of DPPH. Therefore, the chemical composition of the molecule greatly affects its antioxidant activity. Due to its redox characteristics, a certain biopolymer demonstrates significant inhibition of antioxidant activity. The inclusion of hydroxyl and carboxylic groups in natural plant compounds, such as pectin, may aid in the removal of free radicals through scavenging.

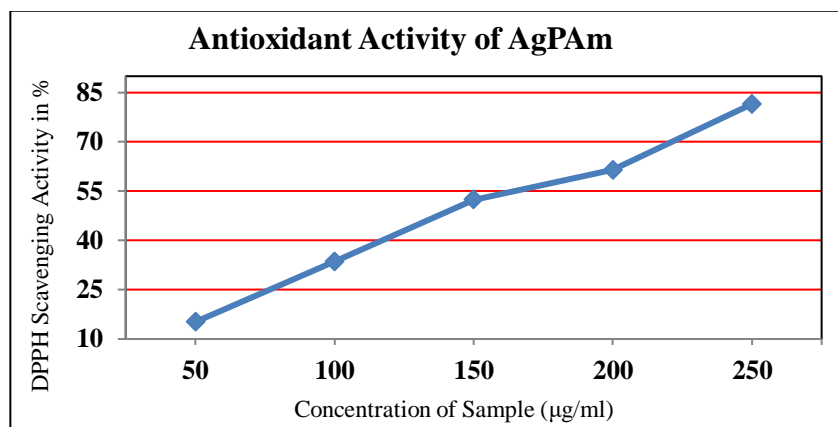


Figure 7. Graph shows the antioxidant activity of synthesized nanogel.

CONCLUSION

In the current research, a copolymerized nanogel composite was synthesized using the chemical polymerization process. The nanogel was synthesized by covalently bonding pectin in a crosslinking network with acrylamide. The nanogel is evaluated using spectroscopy, microscopy, and thermal analysis. The characterizations, including FTIR, DSC and XRD, confirm the crystalline structure, thermal changes, and crosslinking reactions in the formation of functional groups for nanogel. The synthesized nanogel shows a desirable thermal property for DSC as a conductive composite.

Furthermore, the nanogel studies show plausible potential uses for drug delivery systems, such as antibacterial and antioxidant properties. The results indicated that the nanogel had a substantial inhibitory effect on bacterial cells. The Luria bertani agar disc diffusion method was used to assess the copolymer's antibacterial activity against two different concentrations of gram-negative (*Pseudomonas aeruginosa*, *Escherichia coli*) and gram-positive (*Staphylococcus aureus*, *Streptococcus mutans*). The Ngl had a significant effect on *Pseudomonas aeruginosa*, and a potential inhibitory zone was detected. The positive control (azithromycin) had little effect, whereas synthetic nanogel produced a significantly better result. This conclusion demonstrates that the presence of pectin molecules, due to their greater compatibility with bacterial cellular walls, contributes to macromolecule diffusion and association with bacterial cellular walls, as well as preventing cellular wall destruction and growth. The incorporation of silver in the nanogel resulted in a significant enhancement in the antioxidant activity, as indicated by an increased level in the percentage of free radical scavenging ability. Silver-based nanogel could help in the creation of more potent and efficient antioxidants. Hence, this environmentally friendly approach is more cost-effective and practical for the large-scale production of very promising and compatible metal nanogel employing a biological method. It also allows for the investigation of their prospective applications in drug delivery systems by utilizing the surface capping properties of medicinally beneficial plant metabolites.

ACKNOWLEDGEMENT

No financial assistance/grant has been provided to carry out this research work. This research work has been done on a self-financed basis.

CONFLICT OF INTERESTS

The authors declare that there is no conflict of interest.

AUTHOR CONTRIBUTIONS

Each author contributed significantly to this work, reviewed and edited it, and approved the manuscript's publication in its finished form. The authors' ORCID IDs, which are listed below, can be used to confirm their research profiles.

Deepak Ram <http://orcid.org/0009-0007-3534-5681>.

Rohini Dharela <http://orcid.org/0000-0002-8526-7585>.

References

- Haleem, A., Javaid, M., Singh, R. P., Rab, S., & Suman, R. (2023b). Applications of nanotechnology in medical field: a brief review. *Global Health Journal*, 7(2), 70–77. <https://doi.org/10.1016/j.glohj.2023.02.008>.
- Salam, M. A., Al-Amin, M. Y., Salam, M. T., Pawar, J. S., Akhter, N., Rabaan, A. A., & Alqumber, M. a. A. (2023). Antimicrobial Resistance: A Growing Serious Threat for Global Public Health. *Healthcare*, 11(13), 1946. <https://doi.org/10.3390/healthcare11131946>.
- Khalid, M., Amayreh, M., Sanduka, S., Salah, Z., Al-Rimawi, F., Al-Mazaideh, G. M., Alanezi, A. A., Wedian, F., Alasmari, F., & Shalayel, M. H. F. (2022). Assessment of antioxidant, antimicrobial, and anticancer activities of *Sisymbrium officinale* plant extract. *Heliyon*, 8(9), e10477. <https://doi.org/10.1016/j.heliyon.2022.e10477>.
- Dhivya, C., Vandarkuzhali, S. a. A., & Radha, N. (2019). Antimicrobial activities of nanostructured polyanilines doped with aromatic nitro compounds. *Arabian Journal of Chemistry*, 12(8), 3785–3798. <https://doi.org/10.1016/j.arabjc.2015.12.005>.
- Kari, S., Subramanian, K., Altomonte, I. A., Murugesan, A., Yli-Harja, O., & Kandhavelu, M. (2022). Programmed cell death detection methods: a systematic review and a categorical comparison. *Apoptosis*, 27(7–8), 482–508. <https://doi.org/10.1007/s10495-022-01735-y>.
- LoRicco, J. G., Kozel, L., Bagdan, K., Epstein, R., & Domozych, D. S. (2023b). Endosidin 5 disruption of the Golgi apparatus and extracellular matrix secretion in the unicellular charophyte *Penium margaritaceum*. *Annals of Botany*, 131(6), 967–983. <https://doi.org/10.1093/aob/mcad054>.
- Sahoo, S. K., & Labhasetwar, V. (2003). Nanotech approaches to drug delivery and imaging. *Drug Discovery Today*, 8(24), 1112–1120. [https://doi.org/10.1016/s1359-6446\(03\)02903-9](https://doi.org/10.1016/s1359-6446(03)02903-9).
- Wen, N., Lü, S., Xu, X., Ning, P., Wang, Z., Zhang, Z., Gao, C., Liu, Y., & Liu, M. (2019). A polysaccharide-based micelle-hydrogel synergistic therapy system for diabetes and vascular diabetes complications treatment. *Materials Science & Engineering. C, Biomimetic Materials, Sensors and Systems*, 100, 94–103. <https://doi.org/10.1016/j.msec.2019.02.081>.
- Elmowafy, M., Shalaby, K., Elkomy, M. H., Alsaidan, O. A., Gomaa, H. a. M., Abdelgawad, M. A., & Mostafa, E. M. (2023b). Polymeric Nanoparticles for Delivery of Natural Bioactive Agents: Recent Advances and Challenges. *Polymers*, 15(5), 1123. <https://doi.org/10.3390/polym15051123>.
- Kyriakides, T. R., Raj, A., Tseng, T. H., Xiao, H., Nguyen, R., Mohammed, F. S., Halder, S., Xu, M., Wu, M. J., Bao, S., & Sheu, W. C. (2021b). Biocompatibility of nanomaterials and their immunological properties. *Biomedical Materials*, 16(4), 042005. <https://doi.org/10.1088/1748-605x/abe5fa>.
- Shanmuganathan, R., Edison, T. N. J. I., LewisOscar, F., Kumar, P., Shanmugam, S., & Pugazhendhi, A. (2019). Chitosan nanopolymers: An overview of drug delivery against cancer. *International Journal of Biological Macromolecules*, 130, 727–736. <https://doi.org/10.1016/j.ijbiomac.2019.02.060>.
- Winnacker, M. (2017). Polyamides and their functionalization: recent concepts for their applications as biomaterials. *Biomaterials Science*, 5(7), 1230–1235. <https://doi.org/10.1039/c7bm00160f>.
- Sarika, P., & James, N. R. (2015). Preparation and characterisation of gelatin–gum arabic aldehyde nanogels via inverse miniemulsion technique. *International Journal of Biological Macromolecules*, 76, 181–187. <https://doi.org/10.1016/j.ijbiomac.2015.02.038>.
- Papagiannopoulos, A., & Sotiropoulos, K. (2022b). Current Advances of Polysaccharide-Based Nanogels and Microgels in Food and Biomedical Sciences. *Polymers*, 14(4), 813. <https://doi.org/10.3390/polym14040813>.
- Eckmann, D. M., Composto, R. J., Tsourkas, A., & Muzykantov, V. R. (2014). Nanogel carrier design for targeted drug delivery. *Journal of Materials Chemistry. B*, 2(46), 8085–8097. <https://doi.org/10.1039/c4tb01141d>.
- Dheer, D., Arora, D., Jaglan, S., Rawal, R. K., & Shankar, R. (2016). Polysaccharides based nanomaterials for targeted anti-cancer drug delivery. *Journal of Drug Targeting*, 25(1), 1–16. <https://doi.org/10.3109/1061186x.2016.1172589>.
- Soni, K. S., Desale, S. S., & Bronich, T. K. (2016). Nanogels: An overview of properties, biomedical applications and obstacles to clinical translation. *Journal of Controlled Release*, 240, 109–126. <https://doi.org/10.1016/j.jconrel.2015.11.009>.
- Zhang, H., Zhai, Y., Wang, J., & Zhai, G. (2016). New progress and prospects: The application of nanogel in drug delivery. *Materials Science & Engineering. C, Biomimetic Materials, Sensors and Systems*, 60, 560–568. <https://doi.org/10.1016/j.msec.2015.11.041>.
- Wang, H., Qian, J., & Ding, F. (2017). Recent advances in engineered chitosan-based nanogels for biomedical applications. *Journal of Materials Chemistry. B*, 5(34), 6986–7007. <https://doi.org/10.1039/c7tb01624g>.
- Abae, A., Mohammadian, M., & Jafari, S. M. (2017). Whey and soy protein-based hydrogels and nano-hydrogels as bioactive delivery systems. *Trends in Food Science & Technology*, 70, 69–81. <https://doi.org/10.1016/j.tifs.2017.10.011>.
- Caló, E., & Khutoryanskiy, V. V. (2015). Biomedical applications of hydrogels: A review of patents and commercial products. *European Polymer Journal/European Polymer Journal*, 65, 252–267. <https://doi.org/10.1016/j.eurpolymj.2014.11.024>.
- Kim, E. H., Han, G. D., Noh, S. H., Kim, J. W., Lee, J. G., Ito, Y., & Son, T. I. (2017b). Photo-reactive natural polymer derivatives for medical application. *Journal of Industrial and Engineering Chemistry/Journal of Industrial*

- and Engineering Chemistry - Korean Society of Industrial and Engineering Chemistry, 54, 1–13. <https://doi.org/10.1016/j.jiec.2017.05.029>.
23. Bhunia, A. K., Singh, A. K., Parker, K., & Applegate, B. M. (2022). Petri-plate, bacteria, and laser optical scattering sensor. *Frontiers in Cellular and Infection Microbiology*, 12. <https://doi.org/10.3389/fcimb.2022.1087074>.
 24. Masri, A., Brown, D. M., Smith, D. G. E., Stone, V., & Johnston, H. J. (2022b). Comparison of In Vitro Approaches to Assess the Antibacterial Effects of Nanomaterials. *Journal of Functional Biomaterials*, 13(4), 255. <https://doi.org/10.3390/jfb13040255>.
 25. Hasantabar, V., Tashakkorian, H., & Golpour, M. (2019). Fabrication of chitosan based magnetic nanocomposite by click reaction strategy; evaluation of nanometric and cytotoxic characteristics. *Carbohydrate Polymers*, 224, 115163. <https://doi.org/10.1016/j.carbpol.2019.115163>.
 26. Baliyan, S., Mukherjee, R., Priyadarshini, A., Vibhuti, A., Gupta, A., Pandey, R. P., & Chang, C. M. (2022). Determination of Antioxidants by DPPH Radical Scavenging Activity and Quantitative Phytochemical Analysis of *Ficus religiosa*. *Molecules/Molecules Online/Molecules Annual*, 27(4), 1326. <https://doi.org/10.3390/molecules27041326>.
 27. Gulcin, L., & Alwasel, S. H. (2023). DPPH Radical Scavenging Assay. *Processes*, 11(8), 2248. <https://doi.org/10.3390/pr11082248>.
 28. Flieger, J., & Flieger, M. (2020). The [DPPH/DPPH-H]-HPLC-DAD Method on Tracking the Antioxidant Activity of Pure Antioxidants and Goutweed (*Aegopodium podagraria* L.) Hydroalcoholic Extracts. *Molecules/Molecules Online/Molecules Annual*, 25(24), 6005. <https://doi.org/10.3390/molecules25246005>.
 29. Faroudi, L. E., Saadi, L., Barakat, A., Mansori, M., Abdelouahdi, K., & Solhy, A. (2023). Facile and Sustainable Synthesis of ZnO Nanoparticles: Effect of Gelling Agents on ZnO Shapes and Their Photocatalytic Performance. *ACS Omega*, 8(28), 24952–24963. <https://doi.org/10.1021/acsomega.3c01491>.
 30. Li, Y., Liao, Q., Hou, W., & Qin, L. (2023). Silver-Based Surface Plasmon Sensors: Fabrication and Applications. *International Journal of Molecular Sciences*, 24(4), 4142. <https://doi.org/10.3390/ijms24044142>.
 31. Zhao, B., Wu, W., Zhi, J., Su, C., & Yao, T. (2023b). Effect of CeO₂ Content on Melting Performance and Microstructure of CaO-Al₂O₃-SiO₂-MgO Refining Slag. *Metals*, 13(1), 179. <https://doi.org/10.3390/met13010179>.
 32. Ying, S., Guan, Z., Ofoegbu, P. C., Clubb, P., Rico, C., He, F., & Hong, J. (2022b). Green synthesis of nanoparticles: Current developments and limitations. *Environmental Technology & Innovation*, 26, 102336. <https://doi.org/10.1016/j.eti.2022.102336>.
 33. Sharma, P., Sharma, R., Mukhiya, R., Awasthi, K., & Kumar, M. (2021b). Zinc-Oxide based EGFET pH sensors. In Elsevier eBooks (pp. 459–481). <https://doi.org/10.1016/b978-0-12-818900-9.00020-6>.
 34. Zakirov, M. I., Semen'ko, M. P., & Korotchenkov, O. A. (2018b). A Simple Sonochemical Synthesis of Nanosized ZnO from Zinc Acetate and Sodium Hydroxide. *Žurnal Nano- Ta Elektronnoī Fiziki*, 10(5), 05023–05024. [https://doi.org/10.21272/jnep.10\(5\).05023](https://doi.org/10.21272/jnep.10(5).05023).
 35. Kusmus, D. N. M., Van Veldhuisen, T. W., Khan, A., Cornelissen, J. J. L. M., & Paulusse, J. M. J. (2022b). Uniquely sized nanogels via crosslinking polymerization. *RSC Advances*, 12(45), 29423–29432. <https://doi.org/10.1039/d2ra04123e>.
 36. Raj, T., Dharela, R., Vaid, P., & Chauhan, G. S. (2022c). Novel method for extraction of lignin from *Pinus roxburghii* (PR) needles and its application for antimicrobial lignin-silver composite synthesis. *Materials Today: Proceedings*. <https://doi.org/10.1016/j.matpr.2022.09.224>.
 37. Wu, C., Wang, J., Song, S., Wang, Z., & Zhao, S. (2020). Antifouling and anticorrosion performance of the composite coating made of tetrabromobisphenol-A epoxy and polyaniline nanowires. *Progress in Organic Coatings*, 148, 105888. <https://doi.org/10.1016/j.porgcoat.2020.105888>.
 38. Jean, K. D. S., Henderson, K. D., Chrom, C. L., Abiuso, L. E., Renn, L. M., & Caputo, G. A. (2017). Effects of Hydrophobic Amino Acid Substitutions on Antimicrobial Peptide Behavior. *Probiotics and Antimicrobial Proteins*, 10(3), 408–419. <https://doi.org/10.1007/s12602-017-9345-z>.
 39. Reihani, S.F., & Azhar, M.E. (2012). Antioxidant activity and total phenolic content in aqueous extracts of selected traditional Malay salads (Ulam). *international food research journal*, 19, 1439-1444.
 40. Awwad, A. M., Salem, N. M., & Abdeen, A. O. (2013b). Green synthesis of silver nanoparticles using carob leaf extract and its antibacterial activity. *International Journal of Industrial Chemistry./International Journal of Industrial Chemistry*, 4(1), 29. <https://doi.org/10.1186/2228-5547-4-29>.
 41. Zhu, J., Liu, S., Palchik, O., Koltypin, A.Y., & Gedanken, A. (2000). Shape-Controlled Synthesis of Silver Nanoparticles by Pulse Sonochemical Methods. *Langmuir*, 16, 6396-6399.
 42. Locatelli, M., Gindro, R., Travaglia, F., Coisson, J. D., Rinaldi, M., & Arlorio, M. (2009). Study of the DPPH-scavenging activity: Development of a free software for the correct interpretation of data. *Food chemistry*, 114(3), 889-897.
 43. Siddique, M. a. R., Khan, M. A., Bokhari, S. a. I., Ismail, M., Ahmad, K., Haseeb, H. A., Kayani, M. M., Khan, S., Zahid, N., & Khan, S. B. (2024). Ascorbic acid-mediated selenium nanoparticles as potential antihyperuricemic,

- antioxidant, anticoagulant, and thrombolytic agents. *Green Processing and Synthesis*, 13(1). <https://doi.org/10.1515/gps-2023-0158>.
44. Abdel-Rahman, M. A., Alshallash, K. S., Eid, A. M., Hassan, S. E., Salih, M., Hamza, M. F., & Fouda, A. (2024). Exploring the Antimicrobial, Antioxidant, and Antiviral Potential of Eco-Friendly Synthesized Silver Nanoparticles Using Leaf Aqueous Extract of *Portulaca oleracea* L. *Pharmaceuticals*, 17(3), 317. <https://doi.org/10.3390/ph17030317>.
45. Dipankar, C., & Murugan, S. (2012). The green synthesis, characterization and evaluation of the biological activities of silver nanoparticles synthesized from *Iresine herbstii* leaf aqueous extracts. *Colloids and surfaces. B, Biointerfaces*, 98, 112–119. <https://doi.org/10.1016/j.colsurfb.2012.04.006>.